Monatshefte für Chemie 138, 237–244 (2007)
DOI 10.1007/s00706-007-0603-8
Printed in The Netherlands

Monatshefte für Chemie
Chemical Monthly

Intramolecular Hydrogen-Bonding in a C(10)-Exploded Bilirubinoid

Nicholas T. Salzameda and **David A. Lightner***

Department of Chemistry University of Nevada, Reno, USA

Received September 13, 2006; accepted (revised) September 18, 2006; published online February 26, 2007
© Springer-Verlag 2007

Summary. A new linear tetrapyrrole, with two dipyrrinones connected by a string of 5 carbons, was synthesized from two equivalents of a 9*H*-dipyrrinone and one of glutaryl dichloride. Unlike typical dipyrrinones, which are intermolecularly hydrogen bonded in the crystal and in $CHCl_3$ solution, 1,3-bis-[2,3,7,8-tetraethyl-(10*H*)-dipyrrin-9-carbonyl]propane is a monomer in $CHCl_3$, as determined by vapor phase osmometry (VPO) measurements. Its crystal structure determination revealed a folded conformation with a novel type of dipyrrinone to dipyrrinone intramolecular hydrogen bonding. Unexpectedly, the same conformation apparently persists in $CHCl_3$ solution, as shown by ^{1}H NMR spectroscopy.

Keywords. Tetrapyrrole; X-Ray structure; Hydrogen bonding; Vapor pressure osmometry.

Introduction

Dipyrrinones [1] are the yellow component chromophores of bilirubin (Fig. 1A), the linear tetrapyrrole pigment of jaundice. Known to be apprecatious participants in hydrogen bonding, they form ''head-to-tail'' intermolecularly hydrogen-bonded coplanar dimers (Fig. 1B) both in the crystal [2–4] and in nonpolar solvents [4–8]. For example, kryptopyrromethenone (Fig. 1B) was shown to be a dimer in $CHCl_3$ by vapor pressure osmometry (VPO) [5a]. It has a large association constant ($K_A \sim 23000\,M^{-1}$ at 22°C) in chloroform and exhibits lactam and pyrrole NH ^{1}H NMR chemical shifts at 11.42 and 10.44 ppm [7c] respectively. In contrast, the monomer has much more shielded lactam and pyrrole NH chemical shifts: $\delta = 7.75$ and 8.10 ppm, respectively [7c]. These data may be contrasted with those from the polar, hydrogen-bonding solvent $(CD_3)_2SO$ where kryptopyrromethenone, apparently monomeric and hydrogen bonded to solvent [7b], exhibits lactam and pyrrole NH chemical shifts at 9.83 and 10.22 ppm, respectively. When the dipyrrinones are components of a larger molecule and absent the possibility of dipyrrinone to carboxylic acid hydrogen bonding, as in bilirubin dimethyl ester and etiobilirubin-IVγ (Fig. 1C), the tetrapyrrole pigments are dimeric in chloroform [1, 5b, 7a], with a head-to-tail orientation of the intermolecularly hydrogen-bonded dipyrrinones, but not in dimethylsulfoxide, in which the pigments are monomeric and hydrogen bonded to solvent [1, 7b].

In a previous study of the very strong tendency of dipyrrinones to form hydrogen-bonded head-to-tail dimers in nonpolar solvents, we perturbed the stability of the dimer by introducing a butanoyl group at C(9), as in 9-butanoyl-2,3,7,8-tetramethyl-(10*H*)-dipyrrin-1-one (**2**) [8]. With reference to the orientation of the ketone carbonyl at C(10) relative to the adjacent pyrrole NH, there are two limiting conformations of **2** pictured as the two possible hydrogen-bonded head-to-tail dimers of Fig. 2: *syn–syn* (Fig. 2A) and *anti–anti* (Fig. 2B), each with potential dimer-destabilizing elements: in Fig. 2A, electrostatic repulsions between the carbonyls that might weaken the dimer; in Fig. 2B, a steric repulsion between the alkyl fragment of the butanoyl group in one dipyrrinone and the C(2) methyl of the second dipyrrinone. Interestingly, **2** in $CHCl_3$ was shown not

* Corresponding author. E-mail: lightner@scs.unr.edu

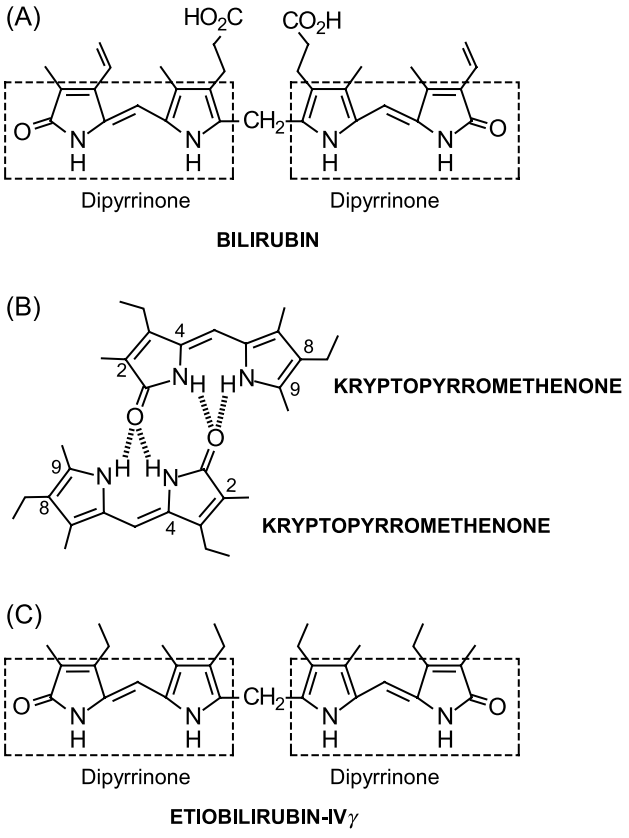

Fig. 1. (A) and (C) Linear representations of bilirubin and etiobilirubin-IVγ, each with two dipyrrinone chromophores. (B) The planar, intermolecularly hydrogen-bonded dimer of kryptopyrromethenone

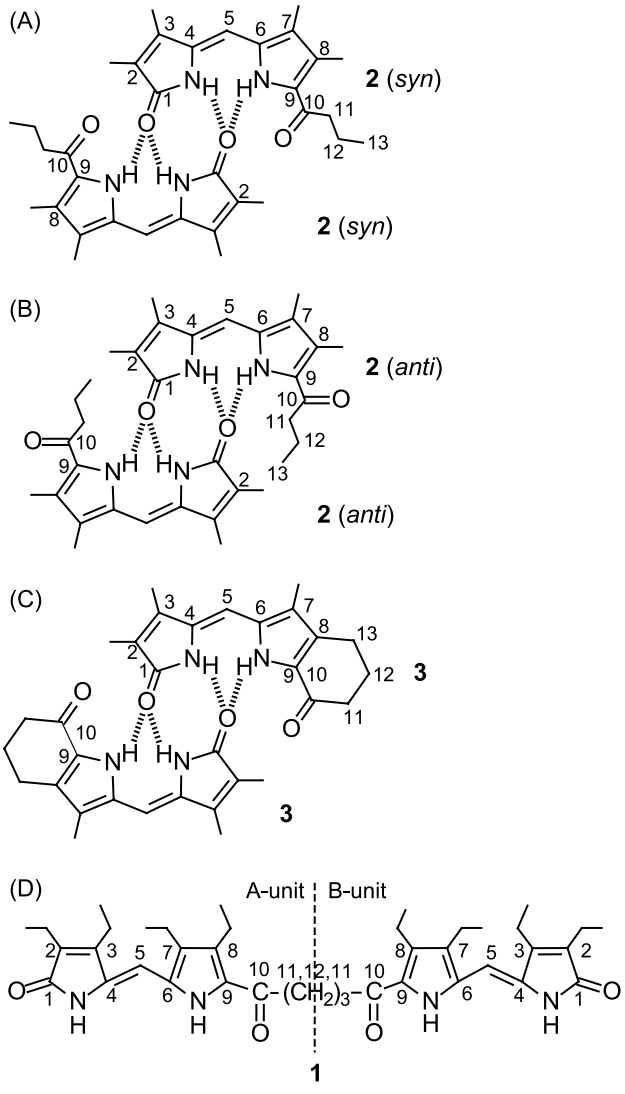

Fig. 2. Head-to-tail hydrogen-bonded dimers of **2** (A) two s*yn*, (B) two *anti* conformations of the butanoyl group of 9-butanoyl-2,3,7,8-tetramethyl-(10*H*)-dipyrrin-1-one (**2**). One can imagine a third dimer (not shown) with one *syn* and one *anti*. The dimer of (A) is found in crystals of **2**, but in $CHCl_3$ **2** is a monomer and adopts the *anti* orientation of (B). (C) Intermolecularly hydrogen-bonded **3**, which has its C(10)=O fixed in the *syn* orientation, as found in $CHCl_3$ solution. (D) Bis-dipyrrinone linear analog **1** (of **2**) and the numbering system used for the A and B dipyrrinones of the X-ray structure

to be a dimer, but monomeric by VPO and ^{1}H NMR, with the butanoyl group oriented in the (*anti*, *ap*) conformation, as may be seen in either of the dipyrrinones in Fig. 2B. The *anti* orientation of the butanoyl apparently is destabilizing toward dimer function because the cyclic analog **3** (Fig. 2C), where the C(10)=O is constrained to be *syn* to the pyrrole NH, forms strong intermolecularly hydrogen-bonded dimers in $CHCl_3$ [8]. In contrast to its behavior in $CHCl_3$, **2** in the crystal is found as an intermolecularly hydrogen-bonded dimer, with both dipyrrinones having the (*syn*, *sp*) orientation of the ketone carbonyl (Fig. 2A) [8]. In other dipyrrinones, particularly those with C(9) alkyl groups (as in Fig. 1B [2] or with 9-H), hydrogen-bonded dimeric structures of dipyrrinones are not unusual and are found in solution as well as in crystal structures.

Intrigued by these findings for **2**, we designed and synthesized a novel linear tetrapyrrole (**1**) where two dipyrrinones are tethered to one another by a short five carbon chain linking C(9) to C(9) (Fig. 2D). Based on the data from **2**, we predicted the possibility of either a dimer or a polymeric string of molecules of **1** in the crystal, linked by intermolecular hydrogen bonds. In $CHCl_3$, we predicted the high probability of a monomeric **1**. Using X-ray crystallography, NMR spectroscopy, and VPO measurements we explored the influence of a C(9)-substituted acyl group on intermolecular association and hydrogen bonding in the crystal and in solution of tetrapyrrole

1 and found unexpected results, as described in the following.

Results and Discussion

Synthesis Aspects and Solution Properties

Following the procedure developed earlier for acylation of 9*H*-dipyrrinones [8], bisdipyrrinone **1** was prepared in acceptable yield by $AlCl_3$-catalyzed *Friedel-Crafts* acylation of 9*H*-dipyrrinone **4** [9] with glutaryl dichloride in CH_2Cl_2, as shown in Fig. 3. Its thin layer chromatographic properties were unusual in that **1** moved faster ($R_f = 0.56$) than **4** ($R_f = 0.31$) with $CHCl_3$-2% CH_3OH eluent, indicating that **1** is unusually nonpolar. It was even less polar than the 9-acyl dipyrrinones **2** ($R_f = 0.31$) and **3** ($R_f = 0.17$), as well as derivatives of **4** with 9-(methyl-1-oxopentanoate) ($R_f = 0.36$) and 9-(1-oxopentanoic acid) ($R_f = 0.39$) groups. Although the observation of a large R_f value for **1** was unusual, we were not surprised to learn that it was a monomer in $CHCl_3$. VPO measurements gave a molecular weight of 642 ± 8 in

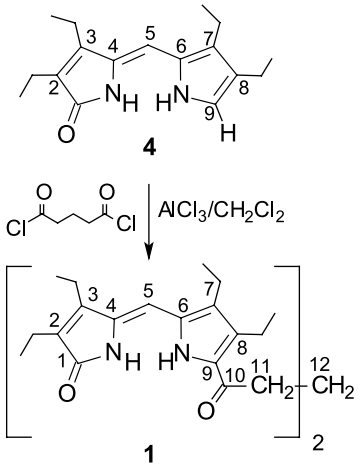

Fig. 3. *Friedel-Crafts* acylation of 2,3,7,8-tetraethyl-(10*H*)-dipyrrin-1-one (4) with glutaryl chloride to afford the target bisdipyrrinone **1**

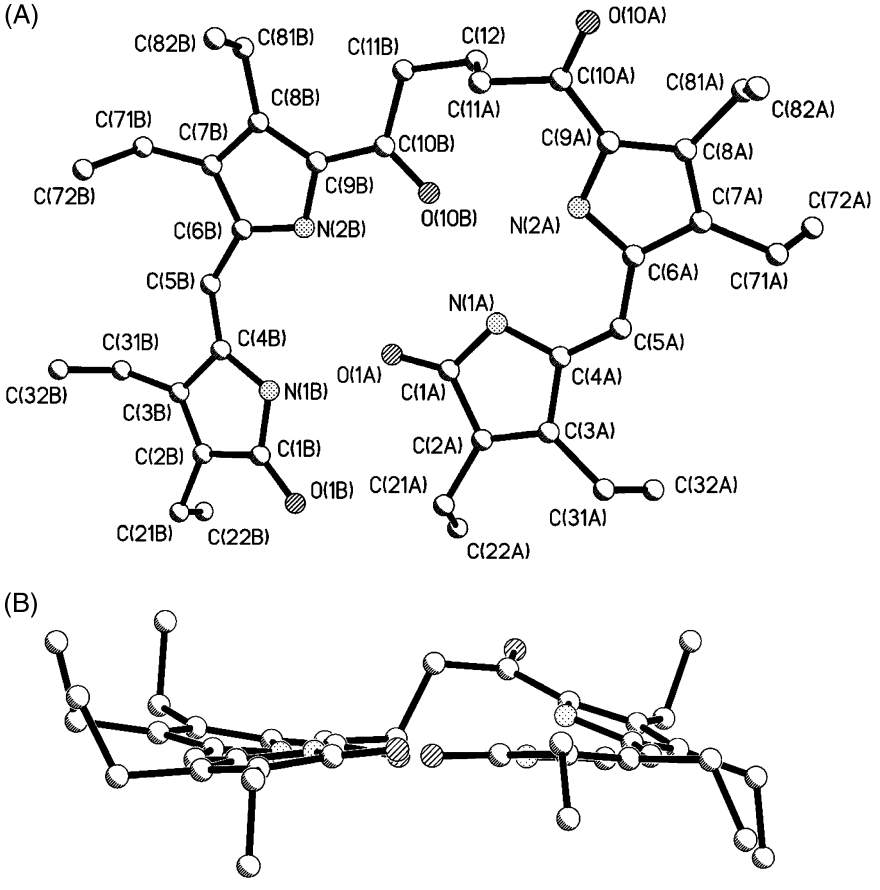

Fig. 4. (A) Structural drawing of **1** (face view) showing the atom numbering scheme used in the X-ray drawings, as observed in its crystal structure. Hydrogens are removed for clarity of representation. The dipyrrinone unit on the left side of the tetrapyrrole (called B) has a *syn* orientation of C=O(10B) and pyrrole N(2B); the dipyrrinone unit on the right side (called A) has an *anti* orientation of its C=(10A) and pyrrole N(2A). (B) Edge view of **1** in the crystal; hydrogens removed

$CHCl_3$, in full accord with the monomer formula weight of 640 g/mol. Thus, like **2**, which is a monomer in $CHCl_3$, but unlike **3** and **4**, which are dimeric, such data firmly establish that **1** is a monomer in $CHCl_3$ solution.

Constitutional Structure, Molecular Geometry, and Hydrogen Bonding in the Crystal

The constitutional structure of **1**, which follows logically from the method of synthesis, was firmly established by X-ray crystallography (Fig. 4). Only one 9-acyldipyrrinone crystal structure determination has been reported [8]; whereas, crystal structures have been obtained from three different dipyrrinones lacking a 9-acyl group [1, 2]. All four dipyrrinones exhibited intermolecular hydrogen bonding in the crystal, with the dipyrrinones paired as in the examples of Figs. 1B and 2A. In contrast, in the solid **1** eschews head-to-tail dipyrrinone-to-dipyrrinone intermolecular hydrogen bonding in favor of a novel type of head-to-head intramolecular hydrogen bonding. To accommodate the unusual intramolecular hydrogen bonding in **1**, as in Fig. 4, the C(10)=O group of one of its component dipyrrinones (call it B) adopts an *sp* orientation, and the C(10)=O of the other (call it A) is oriented *ap*.

The X-ray crystal structure of triclinic **1** shows its individual dipyrrinone units only slightly twisted out of planarity, with a *syn-Z* configuration at C(4)=C(5), and C(4)=C(5)–C(6)–N(2) torsion angles of $-1.7°$ in the *sp* dipyrrinone and 7° in the *ap* dipyrrinone. The closest hydrogen bonding distances between component A and B dipyrrinones (Fig. 3) are best represented by nonbonded N to O distances in the hydrogen bonding region: pyrrole N(2B) to lactam O(1A) = 3.064 Å, lactam N(1B) to lactam O(1A) = 2.816° Å, pyrrole N(2A) to ketone carbonyl O(10B) = 3.352 Å, and lactam N(1A) to ketone carbonyl O(10B) = 2.825 Å. The corresponding hydrogen bond distances, 2.20, 1.96, 2.58, and 2.02 Å, respectively, and the values 2.20 and 1.96 Å are roughly comparable to those of 2-ethylkryptopyrromethenone [2] and are typical of those found in the dipyrrinone dimer of **2** [8]. These nonbonded distances are close to the sum (2.90 Å) of the *van der Waals* radii of N (1.50 Å) and O (1.40 Å). Dipyrrinone B (Fig. 4) with the *sp* orientation of its acyl group has an N(2B)–C(9B)–C(10B)=O(10B) torsion angle of $-3.6°$; whereas, the dipyrrinone (A, Fig. 4) with the *ap* stereochemistry has an N(2A)–C(9A)–C(10A)=O(10A) torsion angle of 169.0°.

Structure from NMR Spectroscopy

With the constitutional structure and unusual conformation of **1** (Fig. 4) firmly established by X-ray crystallography, we explored its conformation in solution. Typically, dipyrrinones and tetrapyrroles are monomeric in $(CD_3)_2SO$. From VPO measurements, we learned that **1** is also a monomer in $CHCl_3$, as is **2** [8], which is unusual for dipyrrinones. The ^{13}C NMR spectrum of **1** in $(CD_3)_2SO$ shows only one set of signals for the two dipyrrinones (A and B), thus indicating that the A and B units found in the crystal are no longer dissymmetric on the NMR time scale. Conversion of 9*H*-dipyrrinone **4** to apparently symmetrical **1** (Fig. 3) leads to (i) new carbon signals in the ^{13}C NMR that are characteristic of the O=C–CH_2–CH_2–CH_2–C=O segment, (ii) loss of the C(9) doublet of **4**, and (iii) shifts in the dipyrrinone ring carbon resonances that correlate well to those of the known 9-butanoyldipyrrinone **2** (Fig. 2) [8]. As expected, the C(9) resonance of **1** shifts downfield, and C(9) of **1** is ~4 ppm more deshielded than in **2** [8] and ~8.5 ppm more deshielded than in **3** [8], where the acyl carbonyl is constrained to the *syn* orientation relative to the pyrrole.

Conformation from NOE Measurements and ^1H NMR Spectroscopy

As revealed by $^1H\{^1H\}$-N*O*E observed between the lactam and pyrrole NHs in $CDCl_3$, both dipyrrinones of **1** and 9-acylated dipyrrinone **2** [8] adopt a *syn-Z* stereochemistry as the most stable conformation [1]. An N*O*E is also seen between the pyrrole NH and the α-CH_2 of the butanoyl chain of **2**, consistent with the *anti* conformation of Fig. 2B in $CDCl_3$ solution [8]. Signficantly, the same sort of N*O*E was observed in **1** – in addition to an N*O*E between the C(8)-ethyl and the other α-CH_2 of the O=C–CH_2–CH_2–CH_2–C=O of the tether (which was not seen in **2**). These data suggest a conformational preference where the C(10) carbonyl group of one dipyrrinone is (i) *anti* or (*ap*) to the pyrrole NH in both **1** and **2** and (ii) *syn* (or *sp*) in the other dipyrrinone **1** (as in **3**). The N*O*E data for **1** in solution are thus consistent with those observed in the crystal and are consistent with the same conformation of **1** in $CDCl_3$ as in the solid.

Table 1. Comparison of the lactam and pyrrole NH chemical shifts[a] of tetrapyrrole **1** with dipyrrinones **2**–**4** and kryptopyrromethenone (**KP**) in $(CD_3)_2SO$ and $CDCl_3$ at 25°C

	$(CD_3)_2SO$		$CDCl_3$	
	Lactam	Pyrrole	Lactam	Pyrrole
1	10.40	10.76	10.50	9.59
2	10.36	10.74	9.33	8.65
3	10.41	11.35	11.09	10.52
4	9.72	10.48	11.05	10.41
KP	9.83	10.22	11.42	10.49

[a] For $10^{-2}\,M$ solutions. Chemical shifts (δ) are reported in ppm downfield from $(CH_3)_4Si$ and referenced to the residual non-deuterated solvent: 7.26 ($CHCl_3$) and 2.49 ppm ($(CD_3)_2SO$). Values for **2**–**4** are from Refs. [8] and [9], for **KP** are from Ref. [7b]

Significantly, in $CDCl_3$ solvent, the ^{1}H NMR **1** shows no structural dissymmetry, *e.g.*, only one set of dipyrrinone signals at room temperature. In the event that **1** might adopt the same hydrogen-bonded structure as in the crystal, it must be in dynamic equilibrium in switching between A and B dipyrrinones on the NMR time scale. Evidence for hydrogen bonding in $CDCl_3$ may be gathered from the NH ^{1}H NMR chemical shifts (Table 1). As expected, the sets of lactam and pyrrole NH chemical shifts of **1** and **2** in dimethylsulfoxide-d_6 are very similar, **1**: $\delta = 10.8$ and 10.4 ppm; **2**: $\delta = 10.7$ and 10.4 ppm for the pyrrole and lactam NHs, respectively. The sets of lactam and pyrrole chemical shifts of **1** and **2** differ markedly in $CDCl_3$, however, **1**: $\delta = 9.6$ and 10.5 ppm; **2**: $\delta = 9.3$ and 8.7 ppm, respectively for the pyrrole and lactam NHs. The greater shieldings in **2** in $CDCl_3$ are consistent with the observation by VPO that **2** is a monomer in chloroform [8] and not engaged in hydrogen bonding; whereas **1**, while monomeric, is engaged in intramolecular hydrogen bonding. Where one finds a dipyrrinone dimer is in **3** (Fig. 2C), an analog of **2** with a cyclohexanone fused at C(9) and C(8) so that the ketone carbonyl is forced to lie *syn* to the pyrrole NH [8]. In **3** the pyrrole and lactam NH chemical shifts in $CDCl_3$ are at 11.1 and 10.5 ppm – values close to the chemical shifts of **1**, and consistent with hydrogen bonding.

From these ^{1}H NMR data showing hydrogen-bonded dipyrrinones in $CDCl_3$, supported by N*O*E studies that indicate the presence of *syn* and *anti* conformations about the C(10)=O, it may be concluded that **1** adopts a solution conformation like that of Fig. 5. Although at 25°C in $CDCl_3$ we do not observe 2 sets of dipyrrinone NH signals that would correlate with a dissymmetric structure for **1**, at −65°C in CD_2Cl_2 we see 2 sets of NH signals, suggesting that while the equilibration between the A and B dipyrrinones is rapid on the NMR time scale at room temperature, it slows at lower temperatures. Thus, in the crystal (Fig. 4) and apparently in solution, **1** adopts a novel conformation where the component dipyrrinones hydrogen bond to one another in an unusual pattern.

UV-Visible Spectral Comparisons

(4*Z*)-Dipyrrinones typically show UV-Vis λ_{max} in the region 380–420 nm, depending on the location, type, and number of substituents. In ordinary dipyr-

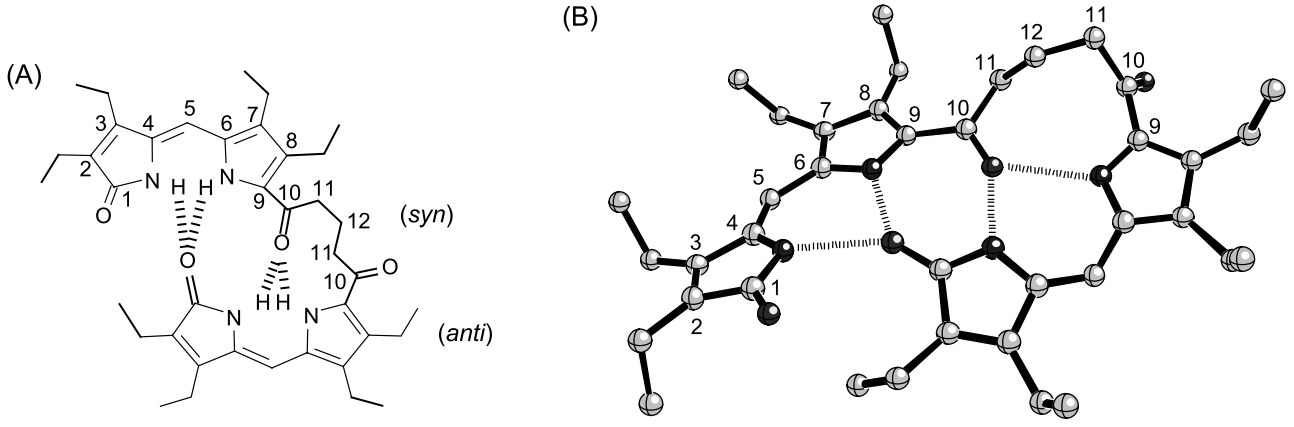

Fig. 5. (A) Unusual head-to-head intramolecular hydrogen bonding observed for **1** in the solid. The C(10)=O and pyrrole N are oriented *syn* in the upper dipyrrinone and *anti* in the lower. (B) Energy-minimized (by molecular dynamics) structure of **1**. Hydrogens are removed for clarity of representation

Table 2. Comparison of the UV-Vis spectral data of bisdipyrrinone **1** with dipyrrinones **2–4** and kryptopyrromethenone (**KP**)

Compound	λ_{max}/nm (ε/mol^{-1} dm^3 cm^{-1})				
	C_6H_6	$CHCl_3$	CH_3CH_3OH	CH_3CN	$(CH_3)_2SO$
1	426 (49700)	425 (47700)^s	421 (46800)	418 (43800)^s	420 (60400)
	399 (76000)	398 (76000)	394 (69200)	391 (72100)	397 (65300)
2	412 (14800)^s	412 (18200)^s	411 (22400)	404 (19400)^s	415 (21800)
	392 (20500)	392 (23700)	392 (28000)	384 (26000)	394 (26200)
3	420 (22200)	413 (16400)^s	415 (24200)	405 (19200)^s	419 (25600)
	397 (27500)	393 (22700)	393 (28000)	386 (24800)	396 (27400)
4	392 (23500)	394 (25300)	396 (27200)	395 (26700)	395 (26300)
KP[a]	–	409 (33900)	416 (39400)	–	415 (35600)

[a] **KP** Kryptopyrromethenone (Fig. 1B) data from *Xie M*, *Lightner DA* (1991) J Heterocyclic Chem **28**: 1753; [s] shoulder

rinones the long-wavelength absorption band lies near 400 nm and is typically intense ($\varepsilon \sim 30000$), as might be expected for a π–π^* type excitation. With an acyl substituent at C(9), as in **1** and **2**, two distinct λ_{max} of roughly equal intensity appear between 390 and 425 nm in all solvents studied (Table 2). The two bands of **2** are not due to an exciton, as there is no evidence for dimer formation in $CHCl_3$ or in the more polar solvents, *e.g.*, $(CH_3)_2SO$, where dimers are not supported. They are also apparently not due to rotational isomers about the acyl group since **3** also exhibits two λ_{max}, and its acyl group is constrained to the *syn* orientation. Comparison of the UV-Vis data for **2** and **3** and their differing λ_{max} and ε values may thus be more a reflection of the differing orientation of the C(10)=O, *syn* in **3**, *anti* in **2**, than the fact that **2** is a monomer and **3** a head-to-tail hydrogen bonded dimer in nonpolar solvents. Except in C_6H_6 and $(CH_3)_2SO$ solvents, one would find it difficult to differentiate between **2** and **3** by UV-Vis spectroscopy. The data also suggest that the C(10)=O group causes the emergence of a second long wavelength electronic transition to complement that seen in simpler dipyrrinones.

In **1**, where the component dipyrrinones are tethered head to head by intramolecular hydrogen bonds, the UV-Vis λ_{max} and ε values (Table 1) do not match up well with those of either **2** or **3**, except that there are two long wavelength bands and the ε values of **1** are approximately twice those of **2** or **3**. The λ_{max} values of **1** are bathochromically shifted by $\sim$15 nm relative to those of **2**, a shift that might be attributed to differing orientations of the C(10)=O relative to the dipyrrinone and more planar dipyrrinones in **1** than in **2**. Molecular modeling [10] studies of **2** predict a C(4)=C(5)–C(6)–N torsion angle of 34°; whereas, in **1** molecular studies (Fig. 5B) predict 11 and 13° in the A and B dipyrrinones. Similarly, the pyrrole N-(9)-C(10)=O torsion angle is $\sim$3° in **2** but more open in the A and B dipyrrinones of **1**: 42 and 21°.

Concluding Comments

Bisdipyrrinone **1**, a C(10) exploded bilirubin analog is intramolecularly hydrogen bonded in the crystal and in $CDCl_3$ solution; with both dipyrrinones adopting *syn-Z* conformations – one with its C(9) acyl substituent oriented *sp*, the other *ap*. Molecular modeling studies [10] indicate that while the typical head-to-tail hydrogen-bonded dimer is possible in **1**, and that (as in **2** [8]) the *sp* conformer is favored in the dimer, intramolecular hydrogen bonding is impossible in either the *sp–sp* or *ap–ap* conformer. In order to accommodate the intramolecular hydrogen bonding, one dipyrrinone adopts the *sp* conformation and the other adopts the *ap* and the *sp–ap* conformation is lowest energy.

Experimental

All UV-Vis spectra were recorded on a Perkin-Elmer λ-12 spectrophotometer, and vapor pressure osmometry (VPO) measurements were performed using an Osmomat 070 (Gonotec, Berlin, Germany) in $CHCl_3$ (from Allied, with amylene stabilizer) at 45°C with benzil used for calibration. Nuclear Magnetic Resonance (NMR) spectra were obtained on a Varian Unity Plus 500 MHz spectrometer in $CDCl_3$ solvent (unless otherwise specified). Chemical shifts were reported in δ ppm referenced to the residual $CHCl_3$ ^{1}H signal at 7.26 ppm and ^{13}C signal at 77.0 ppm. Melting points were taken on a Mel Temp capillary apparatus and are corrected. Combustion analyses were carried out by Desert Analytics,

Tucson, AZ, and gave carbon, hydrogen, and nitrogen percents within 0.30% of theoretical. Analytical thin layer chromatography was carried out on J. T. Baker silica gel IB-F plates (125 μ layer). Radial chromatography was carried out on Merck Silica Gel PF_{254} with gypsum preparative layer grade, using a Chromatotron (Harrison Research, Inc., Palo Alto, CA). Spectral data were obtained in spectral grade solvents. Deuterated solvents were from Cambridge Isotope Labs. Dichloromethane, anhydrous $AlCl_3$, and glutaric acid were from Fisher-Acros. Glutaric acid was converted into its diacid chloride as described previously for diacids [11]. 2,3,7,8-Tetramethyl-(10*H*)-dipyrrin-1-one (4) [9] was prepared by literature methods.

1,3-Bis-[2,3,7,8-tetraethyl-(10H)-dipyrrin-1-one-9-carbonyl]propane (**1**, $C_{39}H_{48}N_4O_4$)

A 500 cm^3 round bottom flask equipped with magnetic stirring was charged with a solution of 0.11 cm^3 glutaryl dichloride and 1.0 g anhydrous $AlCl_3$ in 100 cm^3 CH_2Cl_2, and the mixture was cooled in an ice bath for 10 min. To this solution was added 0.48 g (1.76 mmol) 3,4,7,8-tetraethyl-(10*H*)-dipyrrinone (**4**) [9] in 100 cm^3 CH_2Cl_2, the reaction mixture stirred for 22 h at room temperature, then poured onto ice-water (200 cm^3/100 g) and stirred for 1 h. The organic layer was separated, and the aqueous layer was extracted with CH_2Cl_2 (3×75 cm^3). The combined organic layers were washed with H_2O (4×100 cm^3), then dried over anhydrous Na_2SO_4. The solvent was removed, and the crude product was purified by radial chromatography (97:3 by vol. CH_3OH–CH_2Cl_2) and recrystallization from CH_2Cl_2-*n*-hexane to give pure **1**. Yield: 80 mg (14%); m.p.: 189–190°C; IR (thin film/NaCl): $\bar{\nu} = 2967$, 2933, 2873, 1700, 1670, 1642, 1463, 1433, 1290, 1110, 946 cm^{-1}; ^{13}C NMR ($(CD_3)_2SO$), 125 MHz): $\delta = 189.6$ (C_{10}=O), 172.3 (C_1=O), 146.5 (C_3), 134.0 (C_2), 132.1 (C_8), 131.7 (C_6), 129.6 (C_7), 129.6 (C_9), 128.9 (C_4), 95.9 (C_5), 38.0 (C_{11}), 18.7 (C_{12}), 17.9 (C_{8^1}) 16.9 (C_{2^1}), 16.4 (C_{7^1}), 16.5 (C_{3^1}), 16.3 (C_{8^2}), 15.6 (C_{2^2}), 15.4 (C_{3^2}), 13.6 (C_{7^2}) ppm; ^1H NMR ($(CD_3)_2SO$, 500 MHz): $\delta = 1.14$ (18H, m), 1.21 (t, $J = 7.7$ Hz, 6H), 2.11 (p, $J = 6.9$ Hz, 2H), 2.56 (8H, m), 2.75 (q, $J = 7.7$ Hz, 4H), 2.90 (t, $J = 7.1$ Hz, 4H), 4.76 (q, $J = 7.7$ Hz, 4H,), 6.07 (2H, s), 9.58 (2H, br.s), 10.51 (2H, br.s) ppm; UV-Vis data are in Table 2 .

Table 3. Crystal data and structure refinement for dipyrrinone **1**

Empirical formula	$C_{39}H_{52}N_4O_4$
Formula weight	640.85
Temperature	100(2) K
Wavelength	0.71073 Å
Crystal system	Triclinic
Space group	*P*-1
Unit cell dimensions	$a = 9.008(3)$ Å $\alpha = 92.111(6)°$ $b = 12.238(4)$ Å $\beta = 104.848(6)°$ $c = 17.269(5)$ Å $\gamma = 106.751(6)°$
Volume	1749.4(9) $Å^3$
Z	2
Density (calculated)	1.217 Mg/m^3
Absorption coefficient	0.079 mm^{-1}
F(000)	692
Crystal size	$0.27 \times 0.08 \times 0.07$ mm^3
Theta range for data collection	1.75 to 25.00°
Index ranges	$-10 \le h \le 10$, $-14 \le k \le 14$, $-20 \le l \le 20$
Reflections collected	18456
Independent reflections	6171 [R(int) = 0.0734]
Completeness to theta = 28.27°	99.9%
Absorption correction	SADABS
Max. and min. transmission	0.9947 and 0.9790
Refinement method	Full-matrix least-squares on F^2
Data/restraints/parameters	6171/0/432
Goodness-of-fit on F^2	0.948
Final *R* indices [$I > 2$sigma(I)]	$R1 = 0.0723$, $wR2 = 0.1931$
R indices (all data)	$R1 = 0.0978$, $wR2 = 0.2081$
Largest diff. peak and hole	0.587 and −0.502 e.$Å^{-3}$

X-Ray Structure and Solution

A crystal of **1** was grown by slow diffusion of *n*-hexane into a solution of CH_2Cl_2. A crystal (dimension: $0.27 \times 0.08 \times 0.07$ mm^3) was placed into the tip of a 0.1 mm diameter glass capillary and mounted on a Bruker SMART Apex system for data collection at 100(2) K. A preliminary set of cell constants was calculated from reflections harvested from 3 sets of 20 frames. These initial sets of frames were oriented such that orthogonal wedges of reciprocal space were surveyed (final orientation matrices determined from global least-squares refinement of 18456 reflections for **1**). The data collection was carried out using MoKα radiation (0.71073 Å graphite monochromator) with a frame time of 25 s and a detector distance of 4.94 cm. A randomly oriented region of reciprocal space was surveyed to the extent of 2 hemispheres and to a resolution of 0.84 Å. Four major sections of frames were collected with 0.3° steps in ω at 600 different φ settings and a detector position of 36° for 2θ for **1**. The intensity data were corrected for absorption and decay (SADABS) [12]. Final cell constants were calculated from the *xyz* centroids of strong reflections from the actual data collection after integration (SAINT 6.45, 2003) [13]. Crystal data and refinement information for **1** may be found in Table 3.

The structure was solved and refined using SHELXT-L [14]. The triclinic space group *P*-1 was determined based on systematic absences and intensity statistics. A direct-methods solution was calculated which provided non-hydrogen atoms from the E-map. Full matrix least squares/difference *Fourier* cycles were performed for structure refinement. All non-hydrogen atoms were refined with anisotropic displacement parameters unless stated otherwise. Hydrogen atom positions were placed in ideal positions and refined as riding atoms with relative isotropic displacement parameters (a C–H distance

fixed at 0.96 Å and a thermal parameter 1.2 times the host carbon atom). Tables of atomic coordinates, bond lengths and angles, anisotropic displacement parameters, hydrogen coordinates, and isotropic displacement parameters have been deposited at the Cambridge Crystallographic Data Centre, CCDC No. 619680 for **1**.

Acknowledgements

We thank the U.S. National Institutes of Health (HD-17779) for generous support of this work. *NTS* thanks the NIH for fellowship support. Special thanks are accorded to Prof. *T.W. Bell* for allowing use of the VPO instrument.

References

[1] For leading references, see Falk H (1983) The Chemistry of Linear Oligopyrroles and Bile Pigments, Springer Verlag, Wien

[2] (a) Cullen DL, Black PS, Meyer EF Jr, Lightner DA, Quistad GB, Pak CS (1977) Tetrahedron **33**: 477; (b) Cullen DL, Pèpe G, Meyer EF Jr, Falk H, Grubmayr K (1979) J Chem Soc Perkin **2**: 999; (c) Hori A, Mangani S, Pèpe G, Myer EF Jr, Cullen DL, Falk H, Grubmayr K (1981) J Chem Soc Perkin Trans **2**: 1528

[3] (a) Bonnett R, Davies JE, Hursthouse MB, Sheldrick GM (1978) Proc R Soc London, Ser B **202**: 249; (b) LeBas G, Allegret A, Mauguen Y, DeRango C, Bailly M (1980) Acta Crystallogr, Sect B **B36**: 3007; (c) Becker W, Sheldrick WS (1978) Acta Crystallogr, Sect B **B34**: 1298; (d) Sheldrick WS (1983) Israel J Chem **23**: 155; (e) Mugnoli A, Manitto P, Monti D (1983) Acta Crystallogr, Sect C **C39**: 1287

[4] (a) Tipton AK, Lightner DA (1999) Monatsh Chem **130**: 425; (b) Chen Q, Lightner DA (1998) J Org Chem **63**: 2665

[5] (a) Falk H, Grubmayr K, Höllbacher G, Hofer O, Leodolter A, Neufingerl F, Ribó JM (1977) Monatsh Chem **108**: 1113; (b) Falk H, Schlederer T, Wohlschann P (1981) Monatsh Chem **112**: 199

[6] (a) Boiadjiev SE, Anstine DT, Lightner DA (1995) J Am Chem Soc **117**: 8727; (b) Boiadjiev SE, Anstine DT, Maverick E, Lightner DA (1995) Tetrahedron: Asymmetry **6**: 2253

[7] (a) Kaplan D, Navon G (1983) Israel J Chem **23**: 177; (b) Trull FR, Ma JS, Landen GL, Lightner DA (1983) Israel J Chem **23**: 211; (c) Nogales DF, Ma J-S, Lightner DA (1993) Tetrahedron **49**: 2361

[8] Huggins MT, Lightner DA (2001) Monatsh Chem **132**: 203

[9] (a) Bonnett R, Buckley DG, Hamzetesh D (1981) J Chem Soc Perkin Trans **I**: 322; (b) Huggins MT, Lightner DA (2000) Tetrahedron **56**: 1797

[10] Molecular mechanics and dynamics calculations employed to find the global energy minimum conformations of **1** were run on an SGI Octane workstation using vers. 7.0 of the Sybyl forcefield as described in Refs. [6] and [12]; the Ball and Stick drawings were created from the atomic coordinates using *Müller* and *Falk's* "Ball and Stick" program for Macintosh (http://www.orc.uni-Linz.ac.at/mueller/ball_and_stick.shtml)

[11] Thyrann T, Lightner DA (1996) Tetrahedron **52**: 447

[12] Sheldrick GM (2003) SADABS vers 2.1, Bruker Analytical X-ray Systems, Madison, WI, USA

[13] SAINT vers 6.45 (2003) Bruker Analytical X-ray Systems, Madison, WI, USA

[14] Sheldrick GM (2003) SHELXT-L vers 6.14, Bruker Analytical X-ray Systems, Madison, WI, USA